SI Text: Derivation of thermodynamic parameters from UV-visible and FTIR data

Adopting the scheme from Fig. 1*B*, the transition from Meta I to Meta II_bH^+ is described as a set of three coupled equilibria

$$\text{Meta I} + H^+ \rightleftharpoons \text{Meta II}_a + H^+ \rightleftharpoons \text{Meta II}_b + H^+ \rightleftharpoons \text{Meta II}_b H^+$$

with equilibrium constants

$$\frac{[\text{Meta II}_a]}{[\text{Meta I}]} = K_1, \quad \frac{[\text{Meta II}_b]}{[\text{Meta II}_a]} = K_2, \text{ and } \quad \frac{[\text{Meta II}_b H^+]}{[\text{Meta II}_b][H^+]} = K_3$$

and the normalization $[\text{Meta I}] + [\text{Meta II}_a] + [\text{Meta II}_b] + [\text{Meta II}_b H^+] = 1$.

The concentrations of the individual photoproduct species can be expressed by the equilibrium constants:

$$[\text{Meta I}] = 1/Z, \; [\text{Meta II}_a] = K_1/Z, \; [\text{Meta II}_b] = K_1K_2/Z, \text{ and } [\text{Meta II}_b H^+] = K_1K_2K_3[H^+]/Z,$$

with $Z = 1 + K_1 + K_1K_2 + K_1K_2K_3[H^+]$

Using UV-visible spectroscopy, we determine $\Theta_{\text{UV-vis}}$, the fraction of the photoproducts with deprotonated Schiff base. According to the reaction scheme in Fig. 1*B*, $\Theta_{\text{UV-vis}}$ can be expressed as

$$\Theta_{\text{UV-vis}} = [\text{Meta II}_a] + [\text{Meta II}_b] + [\text{Meta II}_b H^+] = \frac{K_1 + K_1K_2 + K_1K_2K_3[H^+]}{1 + K_1 + K_1K_2 + K_1K_2K_3[H^+]}$$

$$= \frac{K_1 + K_1K_2 + K_1K_2 10^{\text{pKa3}-\text{pH}}}{1 + K_1 + K_1K_2 + K_1K_2 10^{\text{pKa3}-\text{pH}}}$$

with $\text{pK}_{\text{a3}} = -\log_{10}(1/K_3)$. The alkaline endpoint of the UV-vis titration curves is given by

$$\Theta_{\text{UV-vis}}^{\text{alk}} = \frac{K_1 + K_1K_2}{1 + K_1 + K_1K_2}$$

Similarly, we determine by FTIR spectroscopy Θ_{FTIR}, the fraction of the photoproducts with the FTIR signature of an active state conformation. Again, according to the reaction scheme in Fig. 1*B*, Θ_{FTIR} can be expressed as

$$\Theta_{\text{FTIR}} = [\text{Meta II}_b] + [\text{Meta II}_b H^+] = \frac{K_1K_2 + K_1K_2K_3[H^+]}{1 + K_1 + K_1K_2 + K_1K_2K_3[H^+]} = \frac{K_1K_2 + K_1K_2 10^{\text{pKa3}-\text{pH}}}{1 + K_1 + K_1K_2 + K_1K_2 10^{\text{pKa3}-\text{pH}}}$$

and the alkaline endpoint of the FTIR titration curves is given by

$$\Theta_{\text{FTIR}}^{\text{alk}} = \frac{K_1K_2}{1 + K_1 + K_1K_2}$$

The K_i values are obtained by least-squares fits to the spectroscopic observables. With the alkaline endpoint values given above for the UV-vis and FTIR titration curves, this description is equivalent to the description by the phenomenological Henderson-Hasselbalch functions Θ

= $(\Theta^{alk}+10^{pKa-pH})/(1+10^{pKa-pH})$. The apparent pK_a values of these phenomenological Henderson-Hasselbalch titration curves (given in Table S1) are related to pK_{a3} by

$$pK_a = \log_{10}\left(\frac{K_1K_2}{1+K_1+K_1K_2}\right) + pK_{a3}\,.$$

A reduced model was used to derive values for ΔH^o and ΔS^o:

Meta I + H^+ $\rightleftharpoons$ Meta II_b + H^+ $\rightleftharpoons$ Meta II_bH^+

with equilibrium constants

$$\frac{[\text{Meta II}_b]}{[\text{Meta I}]} = K_{12} \text{ and } \frac{[\text{Meta II}_b\text{H}^+]}{[\text{Meta II}_b][\text{H}^+]} = K_3$$

and the normalization $[\text{Meta I}] + [\text{Meta II}_b] + [\text{Meta II}_b\text{H}^+] = 1.$

According to this reduced model, the observables $\Theta_{UV\text{-}vis}$ and Θ_{FTIR} are defined identically as the sum of the concentrations of the Meta II_b and Meta II_{bH}^+ states and are designated as Θ, which is expressed as

$$\Theta = [\text{Meta II}_b] + [\text{Meta II}_b\text{H}^+] = \frac{K_{12}+K_{12}K_3[\text{H}^+]}{1+K_{12}+K_{12}K_3[\text{H}^+]} = \frac{K_{12}+K_{12}10^{pKa3-pH}}{1+K_{12}+K_{12}10^{pKa3-pH}}\,.$$ Using this reduced model, the alkaline endpoint is $\Theta^{alk} = \frac{K_{12}}{1+K_{12}}$.

In this reduced model, the free energy change was calculated as $\Delta G^o_{12} = \Delta H^o_{12} - T\Delta S^o_{12} = -RT \ln K_{12}$, and ΔH^o_{12} and ΔS^o_{12} were obtained from a van 't Hoff analysis over the temperature range from 20 to 37 °C.

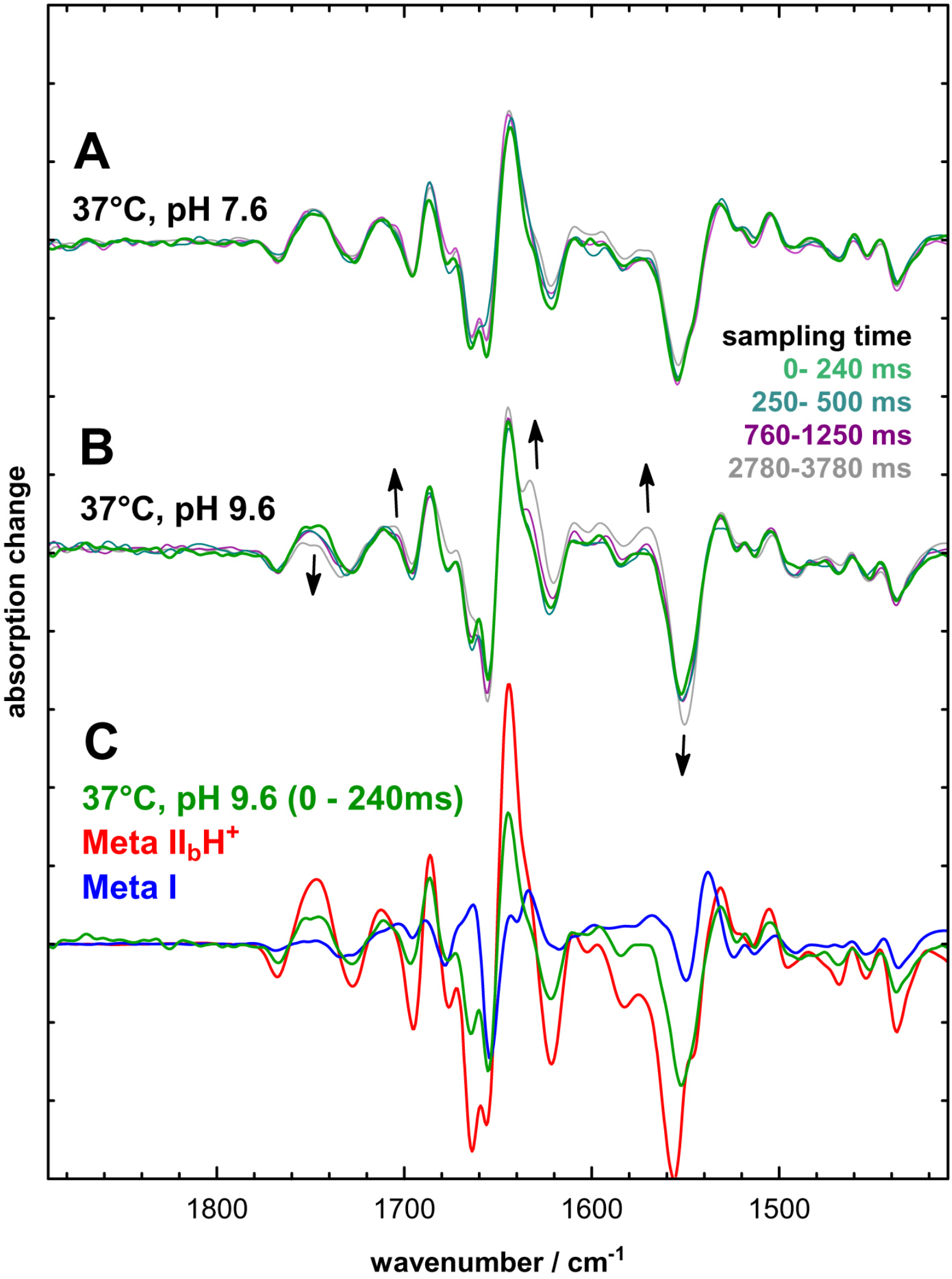
A
37°C, pH 7.6
sampling time
0- 240 ms
250- 500 ms
760-1250 ms
2780-3780 ms
B
37°C, pH 9.6
C
37°C, pH 9.6 (0 - 240ms)
Meta IIbH+
Meta I
absorption change
1800
1700
1600
1500
wavenumber / cm-1

Fig. S1. Confirmation of photoproduct stability in time-resolved FTIR experiments. While the dark state is stable in the range of conditions covered in this study, photoproducts are less stable, in particular at the highest temperature and pH values. To confirm the integrity of the photoproduct states in the difference spectra used for data analysis, the photoproduct spectra were acquired in successive time intervals of approximately 240-ms duration, using quasi-logarithmic averaging for longer time scales. Potential photoproduct decay was assessed using the temporal evolution of spectral marker bands above 1,700 cm^{-1} of membrane-embedded carboxylic acids Glu122 and Asp83 involved in interhelical-hydrogen bonded networks, and of amide I and II marker bands at 1,633 and 1,548 cm^{-1}, respectively, that were characterized in previous studies (1, 2). In order to increase the signal to noise ratio of the difference spectra used for spectral fitting, subsequent post-illumination spectra were averaged over the time range for which no photoproduct destabilization could be observed. (*A* and *B*) Time-resolved photoproduct minus dark state difference spectra that were obtained with rapid-scan FTIR spectroscopy at 37 °C at pH 7.6 and 9.6, respectively. Photoproduct spectra were acquired during time intervals between 0 and 240 ms (green), 250 and 500 ms (turquoise), 760 and 1,250 ms (purple), and 2,780 and 3,780 ms (gray), starting after the 100 ms-photolysis flash. At pH 7.6, the photoproduct remains stable over the entire time range covered in the experiment. At pH 9.6, on the other hand, some destabilization is observed on the longest time scales. Characteristic marker bands of this long-term destabilization are tagged by arrows. (*C*) For data analysis, photoproduct spectra were averaged over time intervals where complete photoproduct stability was warranted by the absence of these spectral changes, which covered, in this particular case, the time interval between 0 and 240 ms. This difference spectrum is decomposed into a linear combination of Meta I and Meta II_bH^+ minus dark state reference spectra.

1. Vogel R, Siebert F (2002) Conformation and stability of α-helical membrane proteins. 2. Influence of pH and salts on stability and unfolding of rhodopsin. *Biochemistry* 41:3536-3545.

2. Vogel R (2004) Influence of salts on rhodopsin photoproduct equilibria and protein stability. *Curr Opin Colloid Interface Sci* 9:133-138.

Table S1. Alkaline endpoint and apparent pK_a values obtained from the phenomenological Henderson-Hasselbalch fit, $\Theta = (\Theta^{alk}+10^{pKa-pH})/(1+10^{pKa-pH})$

Membranes	Temperature, °C	UV-visible		FTIR	
		pK_a	Θ^{alk}_{UV-vis}	pK_a	Θ^{alk}_{FTIR}
Native disk	10	7.1	0	7.2	0
	20	7.7	0.15	7.9	0.15
	30	7.8	0.38	7.8	0.32
	37	7.8	0.58	7.7	0.47
POPC	10	5.7	0	5.7	0
	20	6.0	0.11	6.2	0.08
	30	6.1	0.25	6.2	0.23
	37	5.9	0.46	5.8	0.38

Estimated errors are ±0.05 for Θ values and ±0.2 for pK_a values.